Identification of a Potential Alternative Splicing Prognostic Signature Associated With Immune Infiltrates of Ovarian Cancer

Yan Li
Shengjing Hospital of China Medical University
Yue Han
Shengjing Hospital of China Medical University
Xiaoyin Wang (wangxy5@sj-hospital.org)
Shengjing Hospital of China Medical University https://orcid.org/0000-0002-7908-7617

Primary research

Keywords: ovarian cancer, alternative splicing, prognosis, immune infiltrates, consensus clustering

Posted Date: May 20th, 2021

DOI: https://doi.org/10.21203/rs.3.rs-500677/v1

Abstract

Background: The mortality rate of ovarian cancer (OC) ranks the first in gynecological tumors, which seriously threatens women's health and life. In recent years, alternative splicing (AS) has gradually been considered to play a key role in immune infiltrates of tumor. However, the prognostic significance of AS events related to immune infiltrates in OC remains unknow. The aim of our research was to investigate the potential prognostic value of AS events associated with immune infiltrates in OC.

Methods: The RNA sequences (RNA-seq) and clinical data were downloaded from the Cancer Genome Atlas (TCGA) database. The AS event data was obtained from TCGA SpliceSeq database. Single sample gene set enrichment analysis (ssGSEA) was performed to calculate the abundance of 28 immune cell types in samples from TCGA-OV dataset. A consensus clustering algorithm was used to group the OC patients. Differential expression analysis was used to identify differentially expressed AS events (DEASs) between groups. Univariate Cox regression analysis was implemented to screen for AS events with prognostic value. A least absolute shrinkage and selection operator (LASSO) Cox regression and multivariate Cox regression analyses was used to further narrow the AS events with prognostic value and construct an alternative splicing prognostic signature for predicting the prognosis of OC patients.

Results: The OC patients from TCGA database were classified into two groups (cluster.A and cluster.B) based on the 28 types of TIIC using a consensus clustering algorithm. The patients in the cluster.A group had increased immune infiltrates compared with the cluster.B group. 3616 DEASs were acquired and 171 DEASs have prognostic value ($p<0.05$). 28 DEASs with prognostic value ($p<0.001$) were fitted into LASSO Cox regression and multivariate Cox regression analyses. A prognostic signature with 18 DEASs was constructed to predict the prognosis of OC patients. Each patient obtained a riskscore and the patients were classified into high-and low-risk group using the median riskscore as a cutoff. Kaplan-Meier curve revealed that the patients in high-risk group have poor outcome.

Conclusions: Collectively, our research identified an alternative splicing prognostic signature associated with immune infiltrates of OC, which may provide new directions for the immunotherapy of OC patients.

Introduction

Ovarian cancer (OC) is one of the fatal gynecological malignancies (Swayze et al., 2021). Currently, ovarian cancer is mainly treated by surgery combined with adjuvant chemotherapy and other methods. However, the 5-year survival rate of patients with advanced ovarian cancer is still less than 30% due to surgical limitations, chemotherapy resistance and tumor recurrence and metastasis (Wieser et al., 2018). Therefore, understanding the molecular changes and finding more effective treatments of ovarian cancer is of great significance to improve the survival status of ovarian cancer patients.

In recent years, immunotherapy has attracted much attention as a new approach to cancer treatment, among which programmed cell death receptor-1 (PD-1)/programmed cell death ligand-1 (PD-L1) inhibitor therapy has achieved remarkable efficacy in a variety of tumor treatments (Pawłowska et al., 2019;Fei et

al., 2021). A Pawłowska et al reviewed that PD-1/PD-L1 inhibitors alone or combination therapy showed certain antitumor activity in OC (Pawłowska et al., 2019). However, the appropriate use of PD-1/PD-L1 inhibitors remains a challenge for clinicians. Understanding the formation mechanism of OC microenvironment and finding new predicting methods is essential for the individualization of the OC immunotherapy.

Alternative splicing (AS) refers to the process in which different mature mRNAs are produced from the same mRNA precursors by different splicing and splicing methods. The resulting mRNA is called a transcript, which can then be translated into different protein isomers (Lee and Rio, 2015). AS is an important mechanism to regulate gene expression and produce protein diversity, and it is also an important reason for the great difference in the number of genes and proteins in eukaryotes (Baralle and Giudice, 2017). The Cancer Genome Atlas (TCGA) Spliceseq database provides seven types of AS events: alternate acceptor site (AA), alternate donor site (AD)alternate promoter (AP), alternate terminator (AT), exon skip (ES), mutually exclusive exons (ME), retained intron (RI) (Ryan et al., 2016). Increasing evidence revealed that AS events were associated with the occurrence and development of cancers and act a significant role in the formation of tumor immune microenvironment. (Wan et al., 2019;Qi et al., 2020). However, although there are some researches based on AS events in OC, few studies have comprehensively analyzed the effects of AS events from the perspective of immune infiltrates. Therefore, our research investigated the potential value of AS events associated with immune cell infiltration in OC.

In our study, based on RNA-seq data and clinical information downloaded from the TCGA database, combined with splicing event data obtained from the TCGA Spliceseq database, an efficient and reliable prognostic risk model of OC related to immune infiltrates was constructed. Splicing factor (SF) data were downloaded from SpliceAid 2 database, and the regulatory network between SF and AS events was constructed to lay a foundation for predicting the prognosis of OC patients.

Materials And Methods

Data acquisition

We acquired the RNA-seq data and clinical information of 379 OC patients from the TCGA database (https://portal.gdc.cancer.gov/). The AS events of OC patients was downloaded from the TCGA Spliceseq database (https://bioinformatics.mdanderson.org/TCGASpliceSeq/PSIdownload.jsp), and the splicing percentage (PSI) is obtained. AS events with PSI≥75% were included in this study (Liu et al., 2021). Finally, 403 SF were downloaded from SpliceAid2 database (http://193.206.120.249/splicing_tissue.html).

Single-sample gene set enrichment analysis

Single-sample gene set enrichment analysis (ssGSEA) was used to calculate the abundance of the 28 TIIC types in OC patients from TCGA database. Firstly, we obtained the marker genes of each immune cell type. Next, we searched for these genes in the RNA transcriptome profiles of OC patients from TCGA database. We calculated the abundance of the 28 immune cell types in each sample based on the expression levels of the label genes.

Consensus clustering and differential expression analysis

A consensus clustering algorithm was used to group the OC patients based on the abundance of 28 tumor infiltration immune cell (TIIC) types. The “ConsensusClusterPlus” package in R software was used and 1,000 repetitions were performed to ensure the stability of the classification (Wilkerson and Hayes, 2010). Then, differential expression analysis was performed to identify differentially expressed AS events (DEASs) between groups. The screening criteria was $p<0.05$ and | logFC |.

Construction of a prognostic risk model based on AS events

Univariate Cox regression analysis was used to select the AS events with prognostic value. Then, the AS events with prognostic value were included in Lasso regression for feature selection and dimensionality reduction. 10 fold cross validation was performed 100 repetitions using the “glmnet” package in R software to select the minimum λ value as the best λ parameter value. Finally, we conducted a prognostic risk model through multivariate Cox regression analysis based on the selected AS events. Each patient acquired a riskscore according to the formula: Risk score $=\sum$Coefi × xi (Coefi represents the regression coefficient, xi represents the PSI of AS events). The OC patients were divided into high- and low- risk groups based on the median riskscore.

Construction of the co-expression network between SF and AS events

Pearson correlation analysis was performed to calculate the correlation coefficient between SF and AS events in prognostic risk model. The SF-AS event pairs meet the screening criteria $p<0.05$ and $|R|>0.2$ were selected to conduct the co-expression network. Finally, we visualized the SF-AS event network by cytoscope software.

Statistical analysis

Kruskal-Wallis tests were performed to compare the differences between the groups and p-value<0.05 was considered statistically significant. The “Upset” package in R software was used to visualize the interactive set of the AS events. Kaplan-Meier method was used to draw the survival curve, and Log- rank test was used to evaluate the overall survival rate of patients in the high-risk group and the low-risk group. Receiver operating characteristic (ROC) curves were used to evaluate the predictive power of the prognostic risk model. Univariate and multivariate Cox regression analyses were used to determine whether riskscore was an independent prognostic factor for OC patients.

Results

Identification of differentially expressed AS events related to immune infiltrates

The OC patients from TCGA database were classified using a consensus clustering algorithm based on the 28 types of TIIC. The heatmap showed that the OC patients were divided into two groups (cluster.A and cluster.B, Figure 1A). The patients in cluster.A group have increased immune infiltrates compared with cluster.B group (Figure 1B). We then performed differential expression analysis to select DEASs between cluster.A and cluster.B group. A total of 3616 DEASs were screened out accroding to the screening criteria p<0.05 and | logFC | >0 (Supplementary table 1). The results were visualized using volcano plot and heatmap (Figure 2A and 2B). Upset plot was drew to show the distribution characteristics of DEASs, and the results revealed that ES events were the most common AS events among them, followed by AP and AT events. The vast majority of genes have only one type of AS event, while fewer genes have more (Figure 2C).

Construction of a prognostic risk model based on AS events

Univariate Cox regression analysis was used to identify the prognostic value of the DEASs (Supplementary table 2). 171 AS events with significant prognostic value were selected out accroding to the screening criteria p<0.05 and visualized by volcano plot (Figure 3A). Upset plot also showed that ES events were the most common AS events among the 171 AS events with prognostic value (Figure 3B). Figure 4A-F showed the top 20 AS events with significant prognostic value separately. 28 prognosis-associated AS events with p<0.01 were fitted into LASSO regression to further narrow the AS events to avoid overfitting (Table 1, Figure 5A, B). Finally, 18 AS events were obtained to conduct the prognostic risk model through multivariate Cox regression analysis (Table 2). Each OC patient obtained a riskscore accroding to the formula: Risk score = (-12.8688 × RFTN1|63647|AP) + (-4.02531 × ZNF692|10558|AD) + (1.758544 × FLT3LG|50942|AP) + (-1.3282 × KANK1|85711|AP) + (0.735455 × DMKN|49184|ES) + (1.623249 × ZNF98|48807|AT) + (-0.74984 × SLC10A7|70775|ES) + (-1.72536 × SP140|57870|AT) + (0.906789 × TSGA10|54657|AP) + (-0.92228 × PBRM1|65236|ES) + (1.561355 × SLAIN2|69214|ES) +

(3.065894 × LEF1|70286|AP) + (1.969211 × WDR90|32931|AA) + (0.704623 × LIMS2|55227|AP) + (-4.81758 × COMTD1|186612|ES) + (2.993643 × PAM|72886|ES) + (1.232825 × DCAF11|26847|ES) + (-5.56206 × SMIM7|48188|RI). The OC patients were divided into high- and low- risk group using the median risk score as cutoff. Kaplan–Meier curve indicated that the patients in low- risk group have longer overall survival than in high- risk group (Figure 6A). Furthermore, the AUC value of the ROC curve was 0.765, which revealed that predictive ability of the prognostic risk model was powerful (Figure 6B). From figure 7A and 7B, we found that the mortality of OC patients increased with the risk score. The heatmap showed the distribution of PSI value between high- and low- risk group (Figure 7C).

Independent prognostic value of the prognostic risk model

In order to evaluate whether the prognostic risk model is independent of other clinical information, we conducted univariate and multivariate Cox regression analysis. The clinical variables included age, lymphatic invasion, venous invasion, clinical stage and grade. Univariate Cox regression analysis indicated that age and prognostic risk model was negatively correlated with overall survival of OC patients ($p<0.001$, Figure 8A). After adjustment by multivariate Cox regression analysis, the prognostic risk model was still negatively correlated with the overall survival of OC patients ($p<0.001$, Figure 8B), suggesting that the prognostic risk model was an independent prognostic factor in OC patients.

Construction of the co-expression network between SF and AS events

Abnormal expression of SF is known to interfere with normal splicing of pre-mRNA, leading to abnormal diseases and cancer (Grosso et al., 2008). In order to clarify the complex regulatory relationship between SF and AS events in the prognostic risk model, an interaction network was constructed. Firstly, Pearson correlation analysis was performed to calculate the correlation coefficient between SF and AS events in prognostic risk model. 440 SF -AS event pairs were obtained accroding to the screening criteria $p<0.05$ and $|R|>0.2$ (Supplementary table 3). We revealed the results using cytoscope software (Figure 9).

The predictive property of AS signature was better than mRNA signature

To compare the predictive property of AS signature and mRNA signature, differential expression analysis between cluster.A and cluster.B group was used to select significant mRNAs. 246 significant mRNAs were obtained accroding to the screening criteria $p<0.05$ and $|logFC|>2$ (Supplementary table 4). Then we selected 13 mRNAs with prognostic value from the 246 significant mRNAs using univariate Cox

regression analysis ($p<0.05$, supplementary table 5). 13 prognosis-associated mRNAs were fitted into LASSO regression to further narrow the mRNAs to avoid overfitting (Figure 10 A, B). Finally, 4 mRNAs were obtained to conduct the prognostic risk model using multivariate Cox regression analysis (Supplementary table 6). Each OC patient obtained a riskscore accroding to the formula: Risk score = (7.58E-06 × CYP4F22) +(1.05E-05 × FGF4) + (1.52E-06 ×TMEM59L) + (-1.52E-06× UBD). K-M curve also indicated that the patients in high-risk group have poor outcome than in low-risk group (Figure 10 C). The AUC value of the ROC curve was 0.615, lower than 0.765, suggesting that the predictive property of mRNA signature was poor than AS signature (Figure 10 D).

Discussion

Immune system plays an important role in the occurrence and progression of OC. Immunotherapy can improve autoimmunity, and then effectively prevent and control the occurrence of OC (Rocconi et al., 2020). However, not all patients show the same degree of sensitivity to immunotherapy (Indini et al., 2021). Therefore, the study of the relationship between the immune microenvironment (TME) and the prognosis of OC at the molecular level is of great significance for screening the population with the best benefit from the immunotherapy.

In the present study, ssGSEA algorithm was used to calculate the abundance of the 28 TIIC types in OC patients from TCGA database. Consensus clustering algorithm was implemented to divide the OC patients into two groups (cluster.A and cluster.B) based on the 28 types of TIIC, and the patients in cluster.A have higher immune infiltrates. By comparing the PSI value of AS events between cluster.A and cluster.B, 3616 DEASs related to immune infiltrates were identified. Upset plot revealed that ES events were the most common AS events. Kahles et al (Kahles et al., 2018) showed that although the frequency of AS events was various in different tumor types, the frequency of ES was the highest, which was consistent with our research. Some genes have at least two kinds of AS events, suggesting that AS events play an important role in the occurrence and development of OC. Combining DEASs with survival data, 117 DEASs with significant prognostic value were selected out accroding to the univariate Cox regression analysis. Shanshan Yu et al (Yu et al., 2021) established a prognostic risk model based on the 16 AS events related to immune microenvironment to predict prognosis of Hepatocellular carcinoma (HCC), which may help finding new directions for HCC immunotherapy. In our research, 18 AS events were obtained through LASSO regression to conduct the prognostic risk model using multivariate Cox regression analysis to evaluate the prognostic value of AS events related to immune infiltrates in OC. There was a significant difference between the high- and low- risk group in the prognostic risk model conducted based on the mixed AS events ($P<0.001$). The AUC of the ROC curve was 0.765, suggesting the powerful predictive ability of the prognostic risk model. In order to evaluate whether the prognostic risk model is independent of other clinical variables, univariate and multivariate Cox regression analyses were used. The results indicated that the prognostic risk model was an independent prognostic factor in OC patients ($P<0.001$).

SF plays an important role in the regulation of AS events. Mutation of its nucleic acid sequence or change of its expression level may affect the AS events (Yoshida et al., 2015). However, it is not clear how SF regulates the AS events. Abnormal expression of SF may lead to the formation of specific cancer-promoting shear isomers, leading to the development of cancer (Ge et al., 2019). In order to clarify the complex regulatory relationship between SF and AS events, an interaction network with 440 SF -AS event pairs were established. Among them, 12 AS events and 193 SF was negative correlation, while 12 AS events and 247 SF was positive correlation, indicating that SFs had dual regulatory function and AS events was regulated by different SFs at the same time. Finally, we compared the predictive property of AS signature and mRNA signature, finding that the predictive property of mRNA signature was poor than AS signature, suggesting that AS signature may be better applied in clinical than mRNA signature.

However, we should consider the limitations in this study. Firstly, our data analysis results are only limited to TCGA database due to the lack of AS data in other databases, which may lead to bias. Secondly, due to the incomplete clinical information in the TCGA database, it is not rigorous enough to preliminarily conclude that the risk prognosis model is an independent risk factor for OC patients. Finally, our results are based on pure bioinformatics analysis, lack of corresponding basic or clinical experimental research to verify

Conclusions

In summary, our research conducted a prognostic risk model based on 18 AS events related to immune infiltrates for predicting the prognosis of OC patients, which may be beneficial for screening the population with the best benefit from immunotherapy.

Declarations

Ethics approval and consent to participate

Not applicable

Consent for publication

Not applicable

Availability of data and materials

All data generated or analysed during this study are included in this published article.

Competing interests

The authors declare that they have no competing interests

Funding

Not applicable

Authors' contributions

Yan Li, Yue Han, Xiaoyin Wang conceived and designed the study. Yan Li, Yue Han, Xiaoyin Wang developed the methodology. Yan Li, Yue Han, Xiaoyin Wang analyzed and interpreted the data. wrote, reviewed, and/or revised the manuscript.

Acknowledgments

We thank the authors who provided the TCGA public datasets.

References

1. Baralle FE, Giudice J. Alternative splicing as a regulator of development and tissue identity. Nat Rev Mol Cell Biol. 2017;18:437–51.
2. Fei Z, Xie R, Chen Z, Xie J, Gu Y, Zhou Y, Xu T. Establishment of a Novel Risk Score System of Immune Genes Associated With Prognosis in Esophageal Carcinoma. Front Oncol. 2021;11:625271.
3. Ge Y, Schuster MB, Pundhir S, Rapin N, Bagger FO, Sidiropoulos N, Hashem N, Porse BT. The splicing factor RBM25 controls MYC activity in acute myeloid leukemia. Nat Commun. 2019;10:172.
4. Grosso AR, Martins S, Carmo-Fonseca M. The emerging role of splicing factors in cancer. EMBO Rep. 2008;9:1087–93.
5. Indini A, Nigro O, Lengyel CG, Ghidini M, Petrillo A, Lopez S, Raspagliesi F, Trapani D, Khakoo S, Bogani G. (2021). Immune-Checkpoint Inhibitors in Platinum-Resistant Ovarian Cancer. *Cancers (Basel)* 13.
6. Kahles A, Lehmann KV, Toussaint NC, Hüser M, Stark SG, Sachsenberg T, Stegle O, Kohlbacher O, Sander C, Rätsch G. Comprehensive Analysis of Alternative Splicing Across Tumors from 8,705 Patients. Cancer Cell. 2018;34:211–24.e216.
7. Lee Y, Rio DC. Mechanisms and Regulation of Alternative Pre-mRNA Splicing. Annu Rev Biochem. 2015;84:291–323.
8. Liu J, Lv D, Wang X, Wang R, Li X. Systematic Profiling of Alternative Splicing Events in Ovarian Cancer. Front Oncol. 2021;11:622805.
9. Pawłowska A, Suszczyk D, Okła K, Barczyński B, Kotarski J, Wertel I. Immunotherapies based on PD-1/PD-L1 pathway inhibitors in ovarian cancer treatment. Clin Exp Immunol. 2019;195:334–44.
10. Qi F, Li Y, Yang X, Wu YP, Lin LJ, Liu XM. Significance of alternative splicing in cancer cells. Chin Med J (Engl). 2020;133:221–8.
11. Rocconi RP, Grosen EA, Ghamande SA, Chan JK, Barve MA, Oh J, Tewari D, Morris PC, Stevens EE, Bottsford-Miller JN, Tang M, Aaron P, Stanbery L, Horvath S, Wallraven G, Bognar E, Manning L, Nemunaitis J, Shanahan D, Slomovitz BM, Herzog TJ, Monk BJ, Coleman RL. Gemogenovatucel-T

(Vigil) immunotherapy as maintenance in frontline stage III/IV ovarian cancer (VITAL): a randomised, double-blind, placebo-controlled, phase 2b trial. Lancet Oncol. 2020;21:1661–72.

12. Ryan M, Wong WC, Brown R, Akbani R, Su X, Broom B, Melott J, Weinstein J. TCGASpliceSeq a compendium of alternative mRNA splicing in cancer. Nucleic Acids Res. 2016;44:D1018–22.
13. Swayze EJ, Strzyzewski L, Avula P, Zebolsky AL, Hoekstra AV. (2021). The impact of expanding gynecologic oncology care to ovarian cancer patients in small cities and rural communities. *Gynecol Oncol*.
14. Wan L, Yu W, Shen E, Sun W, Liu Y, Kong J, Wu Y, Han F, Zhang L, Yu T, Zhou Y, Xie S, Xu E, Zhang H, Lai M. SRSF6-regulated alternative splicing that promotes tumour progression offers a therapy target for colorectal cancer. Gut. 2019;68:118–29.
15. Wieser V, Gaugg I, Fleischer M, Shivalingaiah G, Wenzel S, Sprung S, Lax SF, Zeimet AG, Fiegl H, Marth C. BRCA1/2 and TP53 mutation status associates with PD-1 and PD-L1 expression in ovarian cancer. Oncotarget. 2018;9:17501–11.
16. Wilkerson MD, Hayes DN. ConsensusClusterPlus: a class discovery tool with confidence assessments and item tracking. Bioinformatics. 2010;26:1572–3.
17. Yoshida T, Kim JH, Carver K, Su Y, Weremowicz S, Mulvey L, Yamamoto S, Brennan C, Mei S, Long H, Yao J, Polyak K. CLK2 Is an Oncogenic Kinase and Splicing Regulator in Breast Cancer. Cancer Res. 2015;75:1516–26.
18. Yu S, Cai L, Liu C, Gu R, Cai L, Zhuo L. Identification of prognostic alternative splicing events related to the immune microenvironment of hepatocellular carcinoma. Mol Med. 2021;27:36.

Tables

Table1 28 prognosis-associated AS events with p<0.01.

id	z	HR	HR.95L	HR.95H	pvalue
RFTN1|63647|AP	-3.4228	7.20E-06	8.18E-09	0.006342	0.00062
ZNF692|10558|AD	-3.31296	0.004877	0.000209	0.113722	0.000923
FLT3LG|50942|AP	3.259033	7.208535	2.19757	23.64566	0.001118
BCLAF1|77906|ES	3.185595	14.86051	2.824426	78.18749	0.001445
KANK1|85711|AP	-3.06621	0.30424	0.142194	0.650956	0.002168
HK2|54143|AP	-3.05997	0.002277	4.62E-05	0.112197	0.002214
NDUFA3|95376|ES	3.048421	5.429611	1.829589	16.11327	0.0023
LRTOMT|17527|AT	3.044989	12.37772	2.450993	62.50852	0.002327
LRTOMT|17526|AT	-3.04499	0.08079	0.015998	0.407998	0.002327
DMKN|49184|ES	3.034824	2.53259	1.389738	4.61527	0.002407
ZNF98|48807|AT	3.028374	2.585346	1.398095	4.780801	0.002459
ZNF98|48808|AT	-2.99678	0.390629	0.211237	0.722371	0.002729
SLC10A7|70775|ES	-2.99596	0.323053	0.154255	0.676563	0.002736
SP140|57870|AT	-2.95287	0.238901	0.092366	0.61791	0.003148
TSGA10|54657|AP	2.947978	2.955292	1.437876	6.07406	0.003199
TRDMT1|10925|ES	2.898512	3.229025	1.461635	7.133519	0.003749
PBRM1|65236|ES	-2.8833	0.208847	0.072023	0.605597	0.003935
MFAP5|20197|ES	-2.76973	0.039285	0.003976	0.388154	0.00561
SLAIN2|69214|ES	2.767303	5.454143	1.640341	18.13505	0.005652
LEF1|70286|AP	2.75898	55.38988	3.19821	959.2988	0.005798
TBXAS1|81965|AP	-2.73294	0.500879	0.305065	0.822382	0.006277
WDR90|32931|AA	2.731233	15.03227	2.149703	105.1165	0.00631
LIMS2|55227|AP	2.706016	2.237487	1.248618	4.009513	0.00681
COMTD1|186612|ES	-2.66253	0.036626	0.00321	0.417855	0.007756
ARHGEF1|50101|ES	-2.66065	0.190501	0.056161	0.646188	0.007799
PAM|72886|ES	2.644104	10.34182	1.830285	58.43533	0.008191
DCAF11|26847|ES	2.594835	3.886627	1.393956	10.83669	0.009464
SMIM7|48188|RI	-2.57611	0.003786	5.44E-05	0.263492	0.009992

Table2 Regression coefficient of 18 AS events calculated by multivariate Cox regression analysis.

id	coef	HR	HR.95L	HR.95H	pvalue
RFTN1|63647|AP	-12.8688	2.58E-06	1.42E-09	0.004672	0.000774
ZNF692|10558|AD	-4.02531	0.017858	0.000832	0.383083	0.010071
FLT3LG|50942|AP	1.758544	5.803978	1.621187	20.7787	0.006883
KANK1|85711|AP	-1.3282	0.264955	0.11218	0.625789	0.002454
DMKN|49184|ES	0.735455	2.086431	1.064079	4.091042	0.032294
ZNF98|48807|AT	1.623249	5.069534	2.484795	10.34297	8.13E-06
SLC10A7|70775|ES	-0.74984	0.472442	0.215014	1.038077	0.061912
SP140|57870|AT	-1.72536	0.178109	0.065885	0.481487	0.000673
TSGA10|54657|AP	0.906789	2.476358	1.171974	5.232494	0.017515
PBRM1|65236|ES	-0.92228	0.397613	0.11978	1.319882	0.131917
SLAIN2|69214|ES	1.561355	4.765275	1.302232	17.43763	0.018327
LEF1|70286|AP	3.065894	21.45363	0.972357	473.3432	0.052112
WDR90|32931|AA	1.969211	7.165021	0.863528	59.45089	0.068144
LIMS2|55227|AP	0.704623	2.023085	1.030831	3.970458	0.040537
COMTD1|186612|ES	-4.81758	0.008086	0.000606	0.107878	0.000268
PAM|72886|ES	2.993643	19.95825	3.054354	130.4144	0.001773
DCAF11|26847|ES	1.232825	3.430908	1.018035	11.56259	0.046723
SMIM7|48188|RI	-5.56206	0.003841	2.35E-05	0.628994	0.032501

Figures

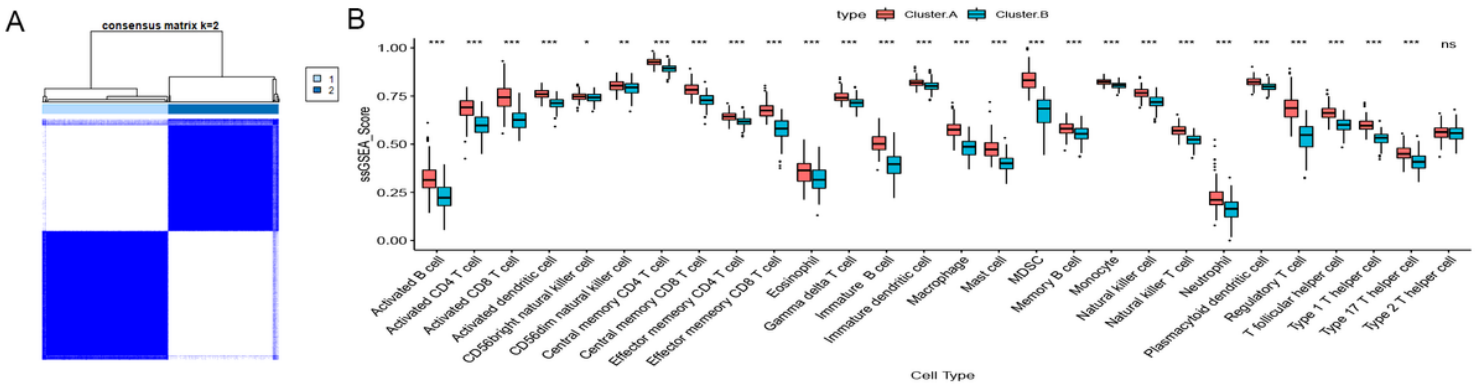

Figure 1

Consensus clustering of the 28 TIIC types. (A) Consensus clustering of the 28 TIIC types. (B) Differential expression histogram of the 28 TIIC types in cluster.A and cluster.B.

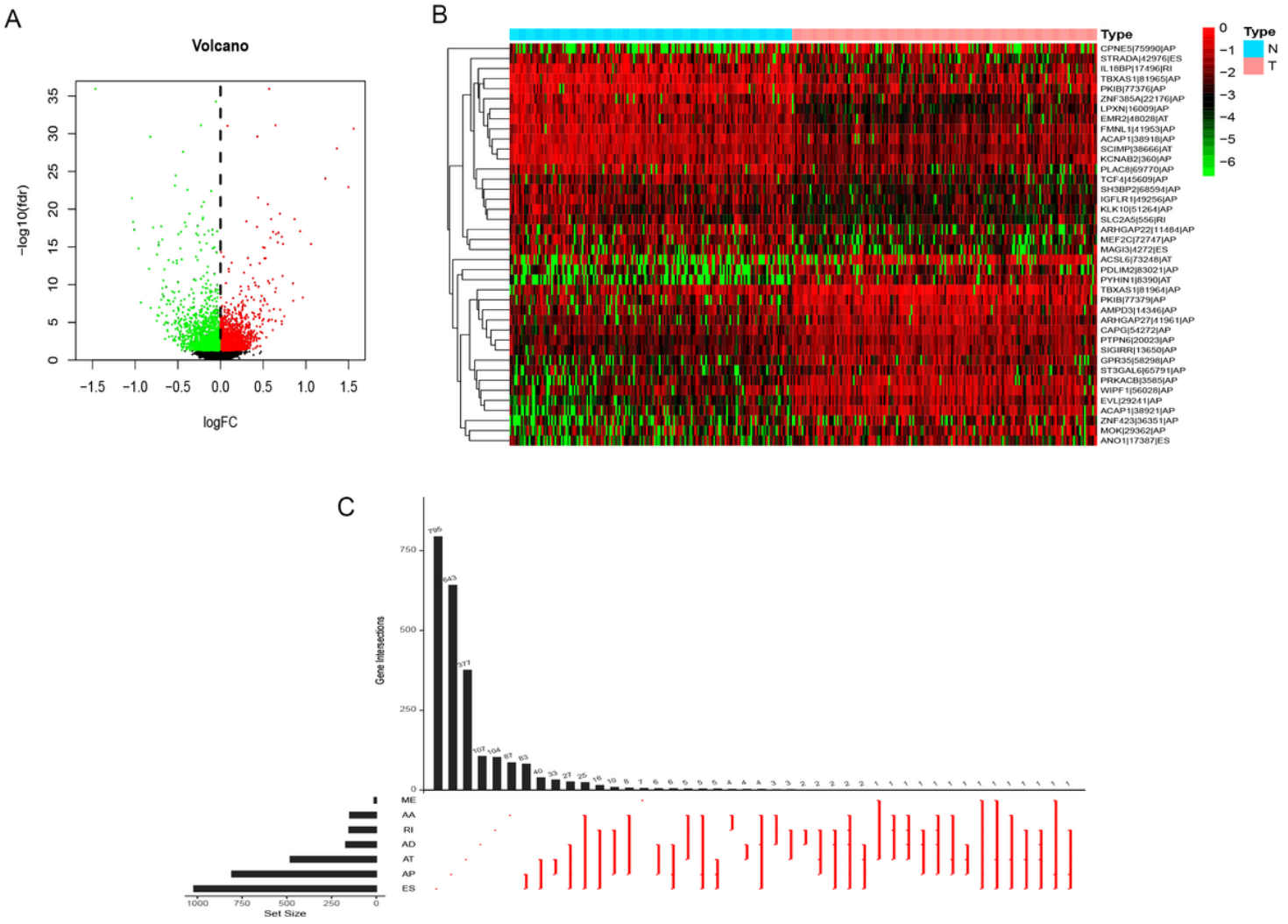

Figure 2

Identification of DEASs related to immune infiltrates in OC. (A) Volcano plots showed the AS event expression between cluster.A and cluster.B group. The red points represent upregulated AS events, while the green points in the plots represent downregulated AS events. (B) Heatmaps showed the top 40 DEASs expression between cluster.A and cluster.B group. The red and green represent higher and lower expression level of AS events, respectively. (C) UpSet plot showed the interactions among the seven types of DEASs.

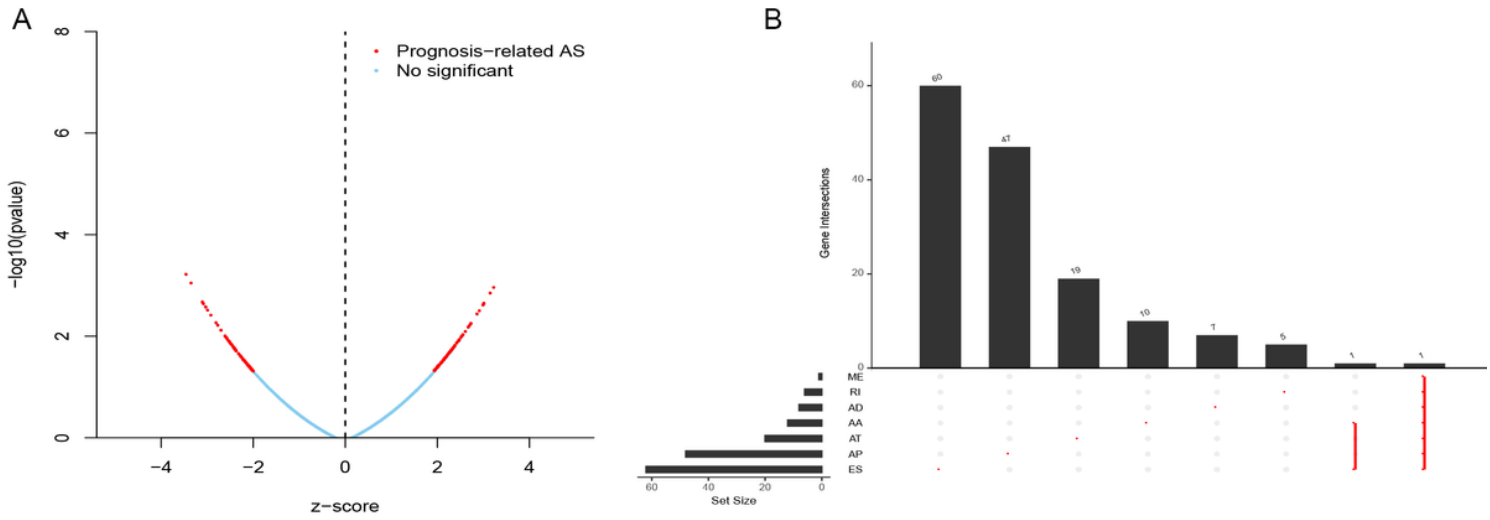

Figure 3

171 AS events with significant prognostic value in OC. (A) The Volcano plot showed the 171 survival-related AS events. The red and green points represent positive and negative correlation with the prognosis of OC, respectively. (B) UpSet plot showed the interactions among the seven types of the 171 survival-related AS events.

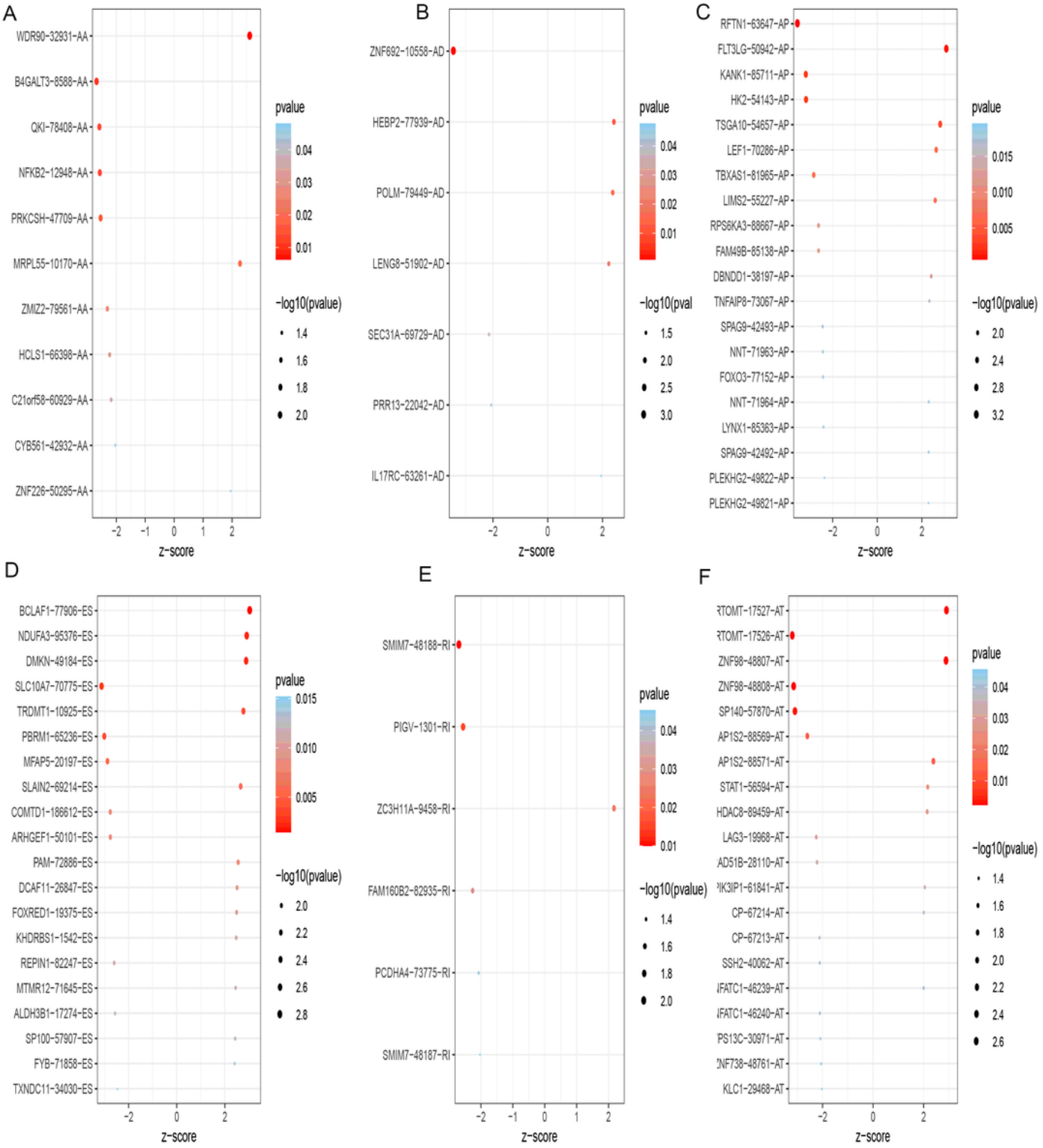

Figure 4

Forest plots of z-score of the top 20 significantly survival-related AS events for seven AS events types. There is no ME event among the 171 survival-related AS events. (A) AA (B) AD (C) AP (D) ES(E) RI (F) AT.

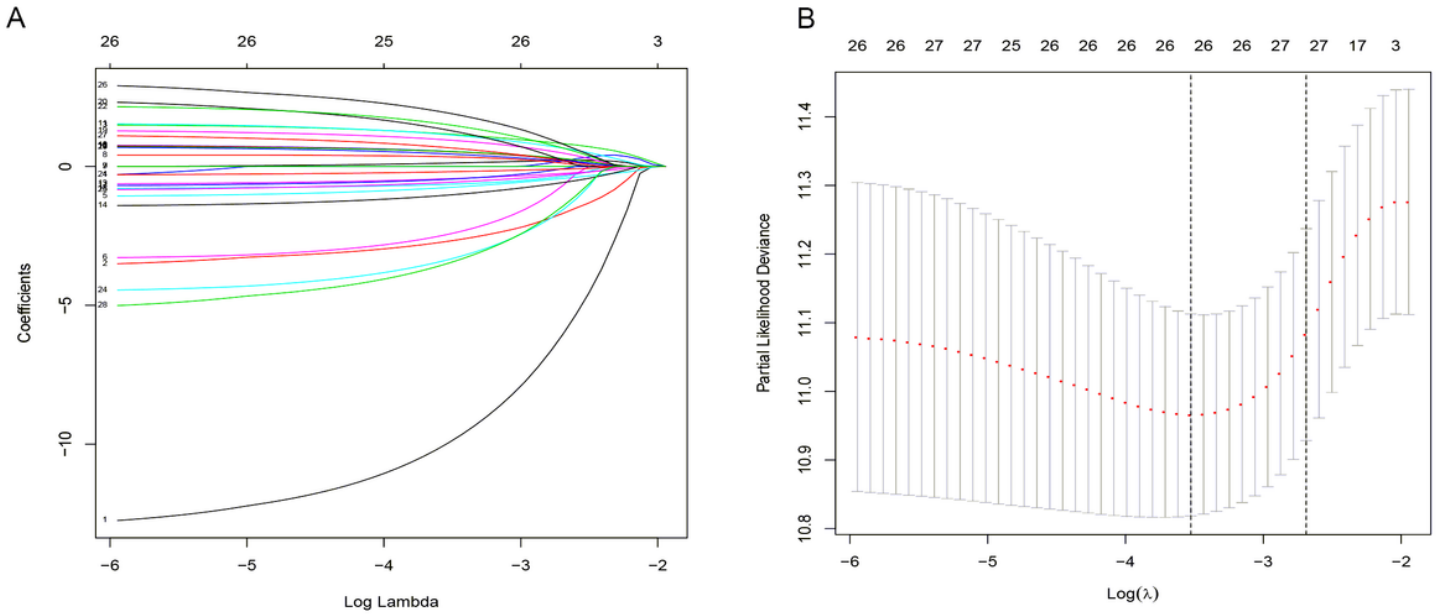

Figure 5

The optimal survival-related AS events were selected by LASSO regression. (A) LASSO coefficient profiles of the171 survival-related AS events. A coefficient profile plot was produced against the log λ sequence. (B) Dotted vertical lines at the optimal values based on the minimum criteria.

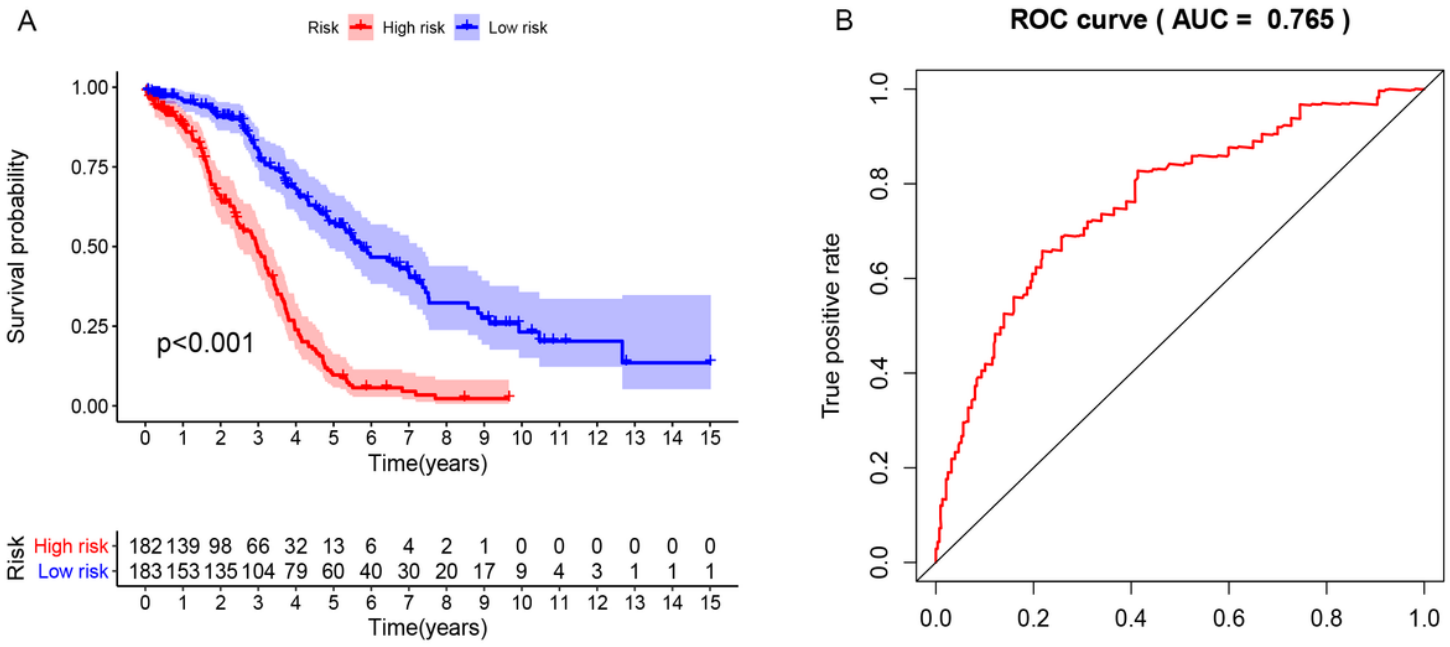

Figure 6

Evaluation of the predictive power of the prognostic risk model based on AS signature. (A) K-M curve to evaluate the survival of patients in high- and low- risk group. (B) ROC curves to evaluate the predictive power of the prognostic risk model.

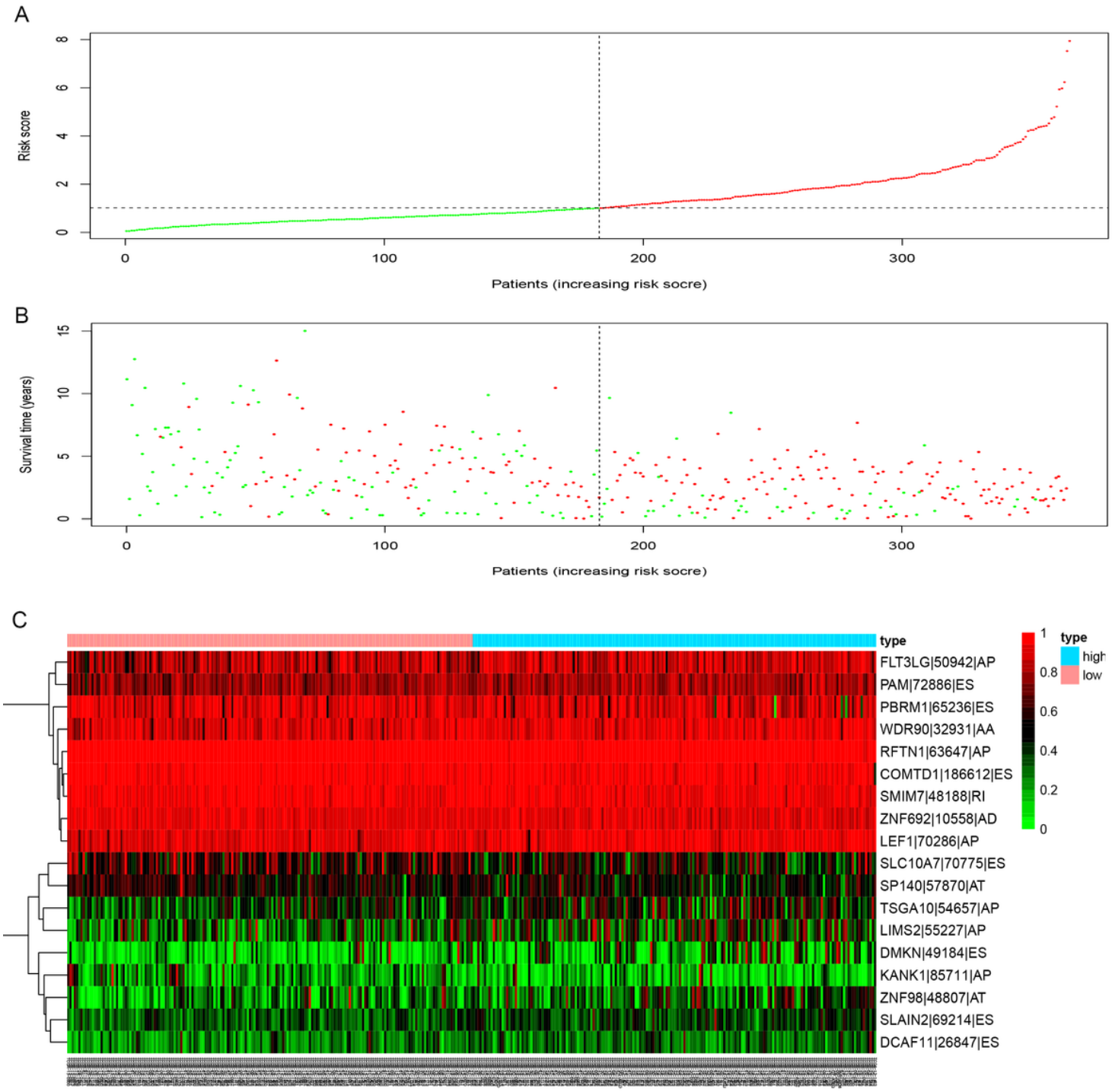

Figure 7

The mortality of OC patients increased with the risk score. (A) Scatter diagram showed the risk score of the 379 OC patients in TCGA database. (B) Scatter diagram showed the survival state of the 379 OC patients in TCGA database. (C) The heatmap showed the distribution of PSI value of the 18 survival-related AS events in high- and low- risk group.

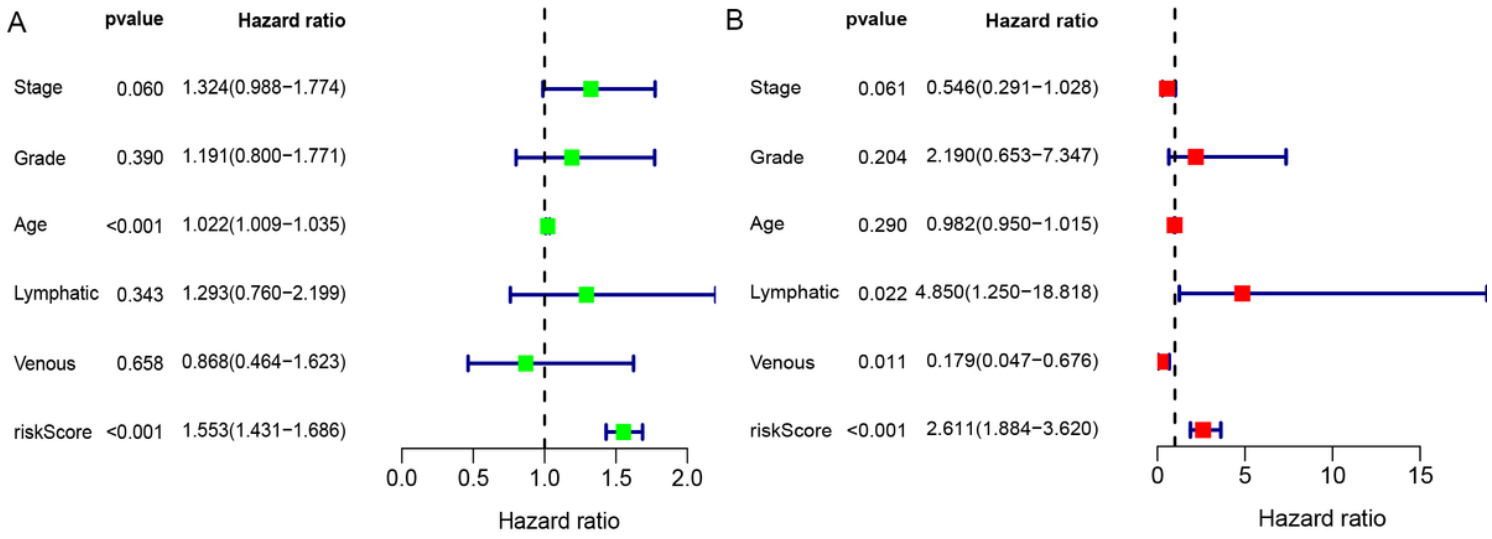

Figure 8

Verification of the independence of the prognostic risk model by univariate and multivariate Cox regression analysis. (A) Univariate Cox regression analyses based on the clinical data and risk score. (B) Multivariate Cox regression analyses based on the clinical data and risk score.

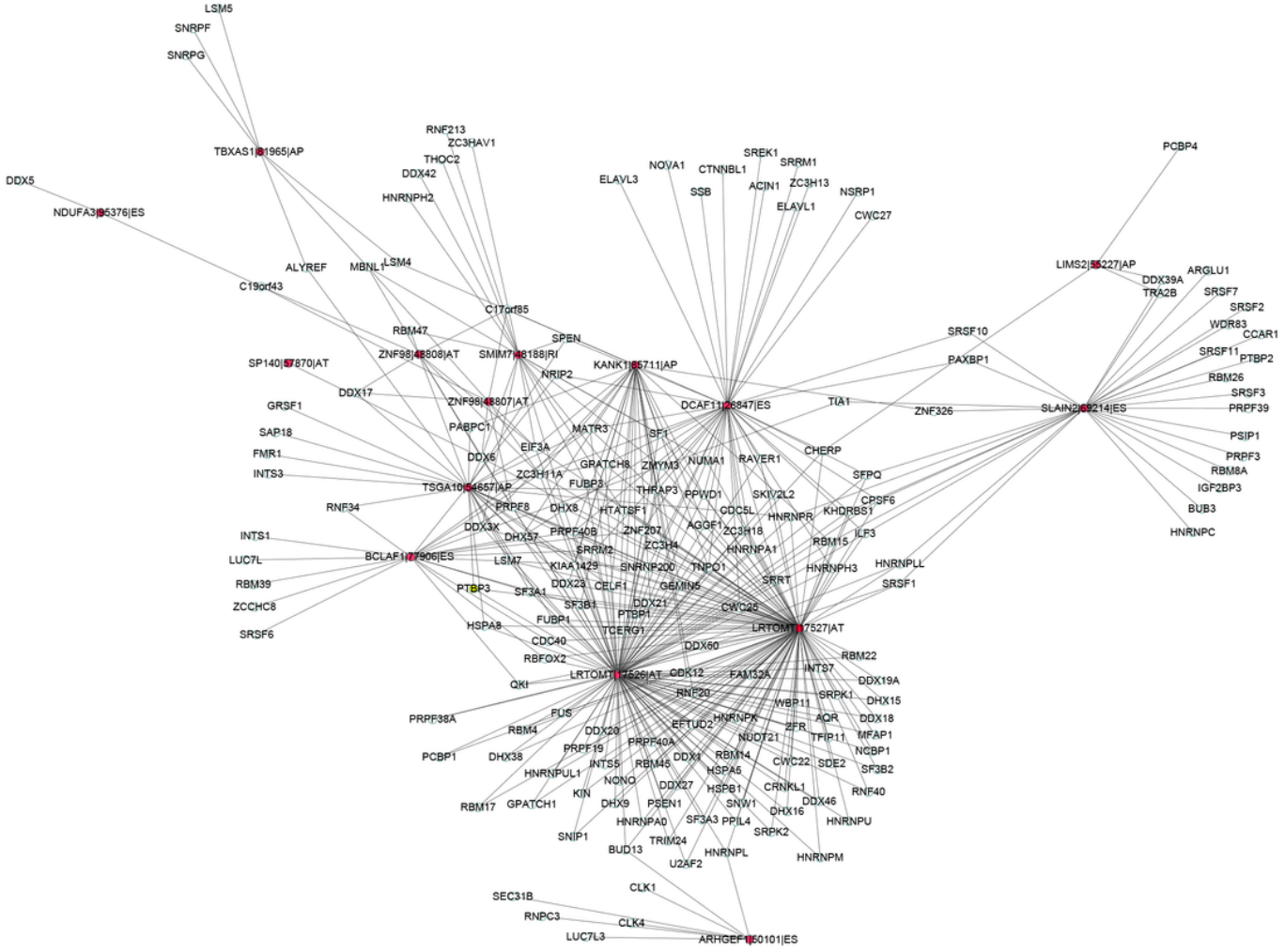

Figure 9

An interaction network with 440 SF -AS event pairs was conducted and visualized by cytoscope software. The red and white points represent AS events and SFs, respectively.

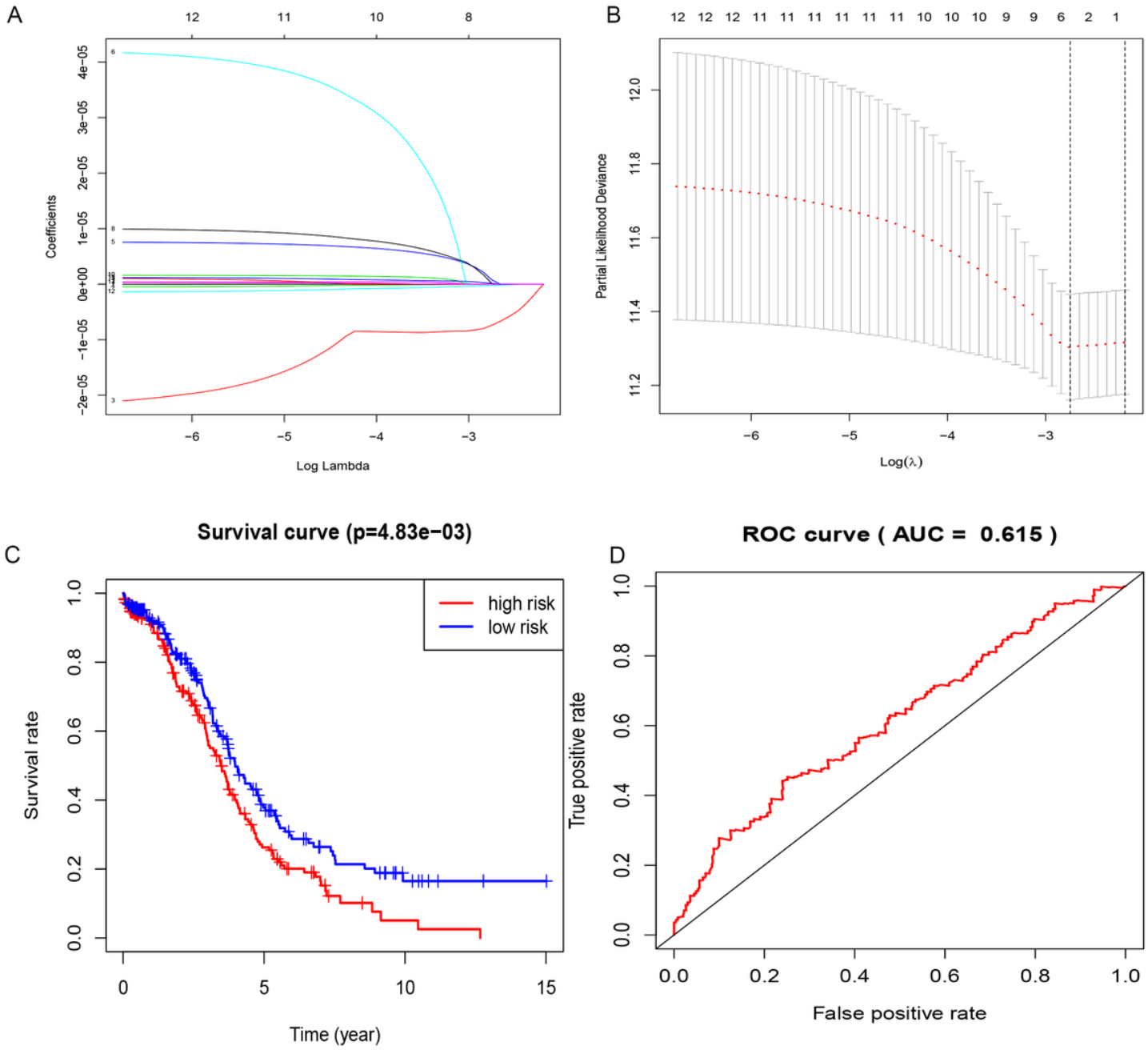

Figure 10

Evaluation of the predictive power of the prognostic risk model based on mRNA signature. (A) K-M curve to evaluate the survival of patients in high- and low- risk group. (B) ROC curves to evaluate the predictive power of the prognostic risk model.

Supplementary Files

This is a list of supplementary files associated with this preprint. Click to download.

- Supplementarytable1.docx

- Supplementarytable2.docx
- Supplementarytable3.docx
- Supplementarytable4.docx
- Supplementarytable5.docx
- Supplementarytable6.docx